

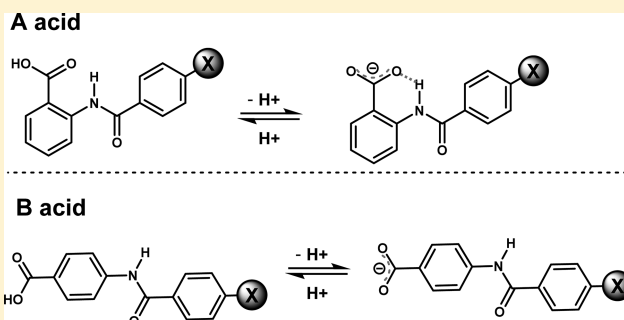
# Substituent Effects on Energetics of Peptide–Carboxylate Hydrogen Bonds as Studied by $^1\text{H}$ NMR Spectroscopy: Implications for Enzyme Catalysis

Bright U. Emenike, Albert Tianxiang Liu, Elsy P. Naveo, and John D. Roberts\*

Gates and Crellin Laboratories of Chemistry, California Institute of Technology, Pasadena, California 91125

**S** Supporting Information

**ABSTRACT:** Substituent effects in  $\text{N}-\text{H}\cdots\text{O}$  hydrogen bonds were estimated by comparing the acidities of two series of model compounds: *N*-benzoylanthranilic acids (**A**) and 4-benzoylamidobenzoic acids (**B**). Intramolecular  $\text{N}-\text{H}\cdots\text{O}$  hydrogen bonds were found to be present in the **A** series of compounds, while **B** acids were used as control models. The respective  $\text{p}K_{\text{a}}$  values for **A** and **B** acids were determined experimentally in DMSO solution using proton NMR spectroscopy. With  $\text{X} = \text{H}$ , the  $\text{p}K_{\text{a}}$  for **A** and **B** acids were observed to be 7.6 and 11.6, respectively, a difference of 4.0 units ( $\Delta\text{p}K_{\text{a}}$ ). However, with  $\text{X} = p\text{-NO}_2$ , the  $\Delta\text{p}K_{\text{a}}$  value between **A** and **B** acids increased to 4.7 units: the  $\text{p}K_{\text{a}}$  values for **A** and **B** acids were determined as 6.7 and 11.4, respectively. The  $\Delta\text{p}K_{\text{a}}$  values between **A** and **B** acids as a function of the  $\text{X}$  substituents were studied in 10 other examples. The effects of  $\text{X}$  substituents in **A** acids could be predicted on the basis of the observed linear Hammett correlations, and the sensitivity of each substituent effect was found to be comparable to those observed for the ionization of substituted benzoic acids ( $\rho = 1.04$  for **A** acids, and  $\rho = 1.00$  for benzoic acids).



## INTRODUCTION

Hydrogen bonding plays a crucial role in enzyme catalysis. The generalized consensus is that the substantial rate enhancements associated with enzyme-catalyzed biochemical transformations partly stem from the myriad of hydrogen bonds provided in the transition states.<sup>1,2</sup> Such stabilization has been estimated to lower the activation barriers of enzyme-catalyzed reactions by  $10 \text{ kcal mol}^{-1}$  or more. On the other hand, non-hydrogen-bonded factors, such as electrostatic and hydrophobic effects, also have been reported to provide enzyme transition state stabilization.<sup>3,4</sup> Despite the apparent importance of hydrogen bonding during biochemical transformation, the exact mechanism at the “reactive site” is still not completely clear. Later, low-barrier hydrogen bonds (LBHBs) were postulated to be responsible for enzyme catalysis,<sup>5</sup> although such a claim is yet to be substantiated. LBHBs are unique hydrogen bonds characterized by strong interaction energies (more than  $10 \text{ kcal/mol}$ ) and downfield  $^1\text{H}$  NMR signals of the hydrogen-bonded protons ( $15\text{--}22 \text{ ppm}$ ). Such LBHBs have been demonstrated in many enzymes’ active site by X-ray crystallographic<sup>6</sup> and proton NMR studies.<sup>7</sup> This evidence led to the suggestion that LBHBs might be involved in enzyme catalysis.<sup>5</sup> For instance, in the active site of  $\alpha$ -chymotrypsin enzyme, Ringe et al.<sup>8</sup> reported a proton NMR chemical shift of  $18.9 \text{ ppm}$  for the low-barrier  $\text{N}-\text{H}\cdots\text{O}$  bond between Asp102 and His57, and the  $\text{p}K_{\text{a}}$  of His57 is  $\geq 12$ , which is 6 units more elevated than the  $\text{p}K_{\text{a}}$  of the imidazole side chain of histidine in water. However, the suggested roles of LBHBs in enzyme catalysis have been heavily criticized.<sup>9–12</sup> Perrin et al. have pointed out that LBHBs are not

very energetic and have joined others in refuting the theory.<sup>9</sup> The fact that experimental measurements of single hydrogen-bond strengths in solution are typically less than  $10 \text{ kcal/mol}$ , as previously calculated by Houk et al.,<sup>13</sup> underscored the premise of the LBHB theory. To the best of our knowledge, reported free energies ( $\Delta G$ ) for the “strongest”  $\text{O}-\text{H}\cdots\text{O}$  hydrogen bonds in solution are within  $8\text{--}11 \text{ kcal/mol}$  ranges.<sup>14,15</sup>

In lieu of the LBHB theory, Shan and Herschlag provided an alternative and more compelling proposal,<sup>16</sup> one that is based on the stabilization attenuated from multiple hydrogen bonds instead of single ones. Despite the modest interaction energies of “normal” single hydrogen bonds ( $\sim 5 \text{ kcal/mol}$ ), recent study by Kass et al.<sup>17</sup> showed that networks of three  $\text{O}-\text{H}\cdots\text{O}$  intramolecular hydrogen bonds in a simple tetraol model (Figure 1) increased the acidity of the tertiary alcohol by a factor of 10.<sup>21</sup> The  $\text{p}K_{\text{a}}$  of the tetraol was determined to be 16.1 in DMSO, whereas *tert*-butyl alcohol (which served as the control model) has a known  $\text{p}K_{\text{a}}$  value of 32.2 in DMSO.<sup>17</sup> The difference in acidity ( $\Delta\text{p}K_{\text{a}} = 16.1$  units;  $\Delta G = 21.9 \text{ kcal/mol}$ ) resulting from the increased stabilization of the charged oxyanion can potentially explain enzymes’ rate enhancement.

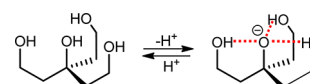


Figure 1. Kass’ tetraol model.

Received: August 15, 2013

Published: October 15, 2013

Moreover, the stabilizing effect of hydrogen bonding has been found to be nearly additive. For example, the single intramolecular O–H...O hydrogen bond in 2-hydroxybenzoic acid (salicylic acid) is responsible for its reduced  $pK_a$  value of 6.6 in DMSO, which is  $\sim 6$   $pK_a$  units lower than the acidity of its isomer (4-hydroxybenzoic acid,  $pK_a = 12.4$ ). On the other hand, 2,6-dihydroxybenzoic acid, which exists with two intramolecular O–H...O hydrogen bonds has a  $pK_a$  value of 3.1, which is  $\sim 10$   $pK_a$  units lower than its intrinsic value of 13.7.<sup>16</sup>

These elegant examples have prompted examination of the origin of the hydrogen-bond effects on the  $pK_a$  of carboxylic acids. In other words, what relationship can we establish between the hydrogen-bond strengths and the ionizability of these acids? In this report, <sup>1</sup>H NMR spectroscopy and quantum mechanical DFT calculations were used to probe the effects of substituent groups on the stabilization of amide N–H...O hydrogen bonds. The importance of substituents in amide hydrogen bonding was demonstrated using a series of small-molecule models derived from *N*-benzoylanthranilic acids (Figure 2). Substituent groups were

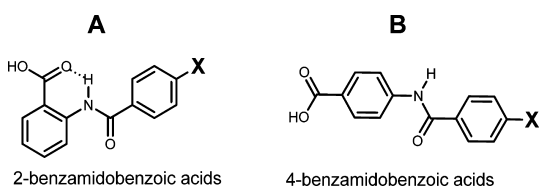


**Figure 2.** Structures of **A** and **B** series of compounds, where the substituent (X) includes a range of electron-donating and electron-withdrawing substituents.

found to have substantial influences on hydrogen-bond strength by changes in the acidity of the benzoic acids.

## RESULTS AND DISCUSSIONS

In previous studies, salicylic acids have been demonstrated to be valuable model systems for investigating O–H...O intramolecular hydrogen bonds.<sup>16,18–20</sup> The replacement of the hydroxyl group with an amide has also proven beneficial in the study of N–H...O interaction.<sup>21</sup> The improvement of the new series (1–12, Figure 3) results from electronegatively changing

the hydrogen bond donor (–NH) using a range of electron-donating and electron-withdrawing substituents. By placing the substituent groups on the benzamide ring and not on the benzoic acid ring, the emphasis of the substituents' electronic influence is placed on the acidities of each compound's NH proton. Because the carboxylic group is farther away from the substituent than the amide group, changes in the acidities of the carboxylic acids as a function of substituent groups should occur primarily as a result of the plausible hydrogen bonding between the amide and carboxyl functional groups. In order to test these hypotheses, we also considered a second set of para-substituted benzoic acids as control compounds **B** (13–16). Note that the differences between the acidities of ortho-substituted benzoic acids (such as **A**) and para-substituted benzoic acids (such as **B**) previously have been used to provide quantitative measures of hydrogen bonding in DMSO.<sup>16,18</sup>

### Intramolecular N–H...O Hydrogen Bonds in Solution.

DMSO is a polar aprotic solvent with a smaller dielectric constant than water (i.e.,  $\epsilon = 46.7$  vs 78.4); it has been commonly used as a crude model to mimic the interior of enzymes' hydrophobic active sites. The proton NMR spectroscopic approach was used largely because of its sensitivity in detecting N–H...O hydrogen bonding in solution, particularly in aprotic solvents.<sup>22</sup> In general, for the series of model systems **A** (1–12), the NH proton appeared to be broadened and centered around 13.5 ppm in DMSO, where **12** exhibited the most downfield chemical shift (13.9 ppm), not surprisingly by having a CF<sub>3</sub> group directly attached to the amide carbonyl group. In contrast, **3** was also electron attracting, but its influence was diminished by having a 4-trifluoromethylphenyl. For the control model **B** (13–16), the –NH proton shifts were  $\sim 10.5$  ppm, indicating a chemical shift difference of 3 ppm relative to model systems **A**. The differences in the chemical shifts between **A** and **B** are much more profound in the monoanions where these compounds exist as carboxylates. Thus, for the monoanion of **12**, the <sup>1</sup>H NMR signal of the NH proton shifted further downfield from 13.9 to 18.4 ppm, whereas that of the **13** monoanion for example, remained essentially the same (i.e., from 10.6 to 10.5 ppm). The further downfield chemical shifts for the NH proton observed in **12**-monoanion is typical of a "low barrier" hydrogen bond in which the bridging proton has

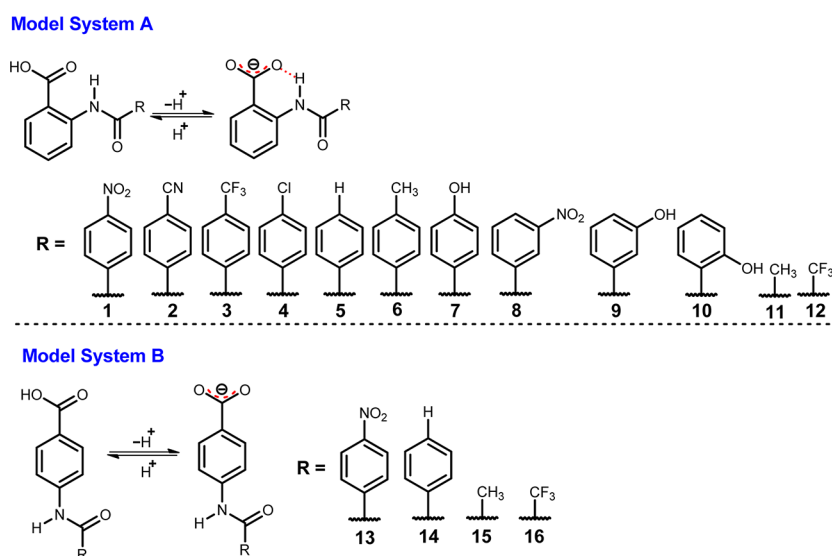


**Figure 3.** Scheme showing model compounds **A** (1–12) and **B** (13–16).

become deshielded from the N electrons as a result of N–H bond elongation (Figure 4). The apparent chemical shift difference for the NH signals in the carboxylates of **12** and **13** (~8 ppm i.e., 18.4 vs 10.5 ppm) shows that model systems **A** are stabilized by N–H···O hydrogen bond, whereas the **B** controls are not. The comprehensive NH proton chemical shifts for the respective monoanions of model system **A** are listed in Table 1.

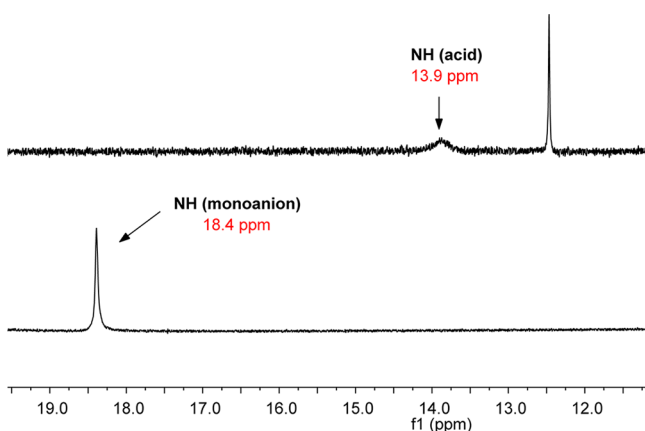


**Figure 4.**  $^1\text{H}$  NMR signal showing the NH region for the acid **12** (top), and its monoanion (bottom) in  $\text{DMSO}-d_6$  solvent.

The 18.4 ppm for the bridging NH proton is consistent with the occurrence of LBHBs in solution and agrees with the experimental value of 18 ppm reported for chymotrypsin and trypsin.<sup>23</sup>

**Conformational Analysis for Model System A.** To further understand the structural geometry of the N–H···O hydrogen bond, conformational search calculations were performed. Molecular mechanics calculation using the Spartan program (MMFF94) produced two low-energy conformers for **12**. These conformers were subsequently reoptimized by density functional theory (DFT) methods at the B3LYP/6-31+G(d) level<sup>17</sup> to give two stable conformers **12a** and **12b** (Figure 5). The relative free energies realized through vibrational frequency calculations at the IEFPCM/B3LYP/6-311+G(d,p) levels (solvent = DMSO)<sup>17</sup> predicted conformer **12a** to be more stable by 2.4 kcal/mol. Interestingly, similar calculations for the monoanion (**12**-monoanion) revealed a deshielded N-proton because the N–H bond was 0.06 Å longer than that of the acid (i.e., 1.08 Å vs 1.02 Å). This finding is

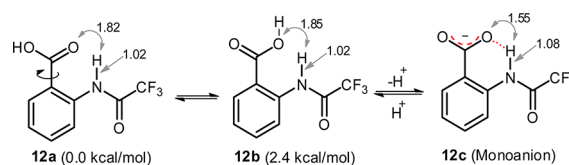


**Figure 5.** Low-energy conformers and the relative free energy for compound **12** computed at B3LYP/6-311+G(d,p)//B3LYP/6-31+G(d) level. The selected O···H distances are calculated values in Å.

congruent with the occurrence of the 18.4 ppm downfield chemical shift observed in the  $^1\text{H}$  NMR spectrum. In addition, the calculated H···O distance in the **12**-monoanion (1.55 Å) was substantially shorter than those for the acid (1.82 Å for **12a**, and 1.85 Å for **12b**). Both the DFT calculations and the  $^1\text{H}$  NMR results seem to support the idea of strong hydrogen bonding in model system **A**.

An X-ray crystal structural analysis was obtained for the crystalline **1** (shown in Figure 6). The solid state also indicated

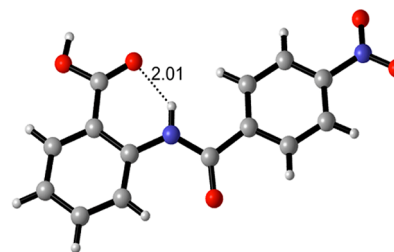


**Figure 6.** X-ray crystal structure of **1** crystallized from  $\text{CH}_2\text{Cl}_2$  solution; shown distance is in Å.

that N–H···O hydrogen bond is quite possible because the N–O (2.68 Å) is shorter than the sum of the van der Waals radii between a nitrogen and an oxygen atom (3.07 Å). Therefore, the NH proton is located within the van der Waals distance necessary for N–H···O hydrogen bonding. In addition, the H···O distance of 2.01 Å is less than the 2.72 Å sum of the van der Waals radii between hydrogen and oxygen atoms.

**Substituent Effects on Hydrogen Bond Strength and Acidity ( $\text{p}K_a$ ).** Because model system **A** indeed appears to form intramolecular hydrogen bonds in DMSO solutions and also because the presence of intramolecular hydrogen bond is expected to perturb the acidity of the benzoic acid, it appears

**Table 1.** (–NH) Chemical Shifts of the Monoanions, Ionization Constants ( $K_a$ ), and Hydrogen Bond Interaction Free Energies for Compounds **1**–**12** in  $\text{DMSO}-d_6$

compd	R	$\sigma_x^a$	$\delta_{\text{NH}}$ (ppm)	$\text{p}K_a$	$K_{\text{obs}}$	$\Delta G$ [kcal/mol]
1	( <i>p</i> -NO <sub>2</sub> )-Ph	0.78	16.6	6.7 ± 0.2	2.00 × 10 <sup>−7</sup>	−6.7
2	( <i>p</i> -CN)-Ph	0.66	16.2	6.9 ± 0.1	1.25 × 10 <sup>−7</sup>	−6.4
3	( <i>p</i> -CF <sub>3</sub> )-Ph	0.54	16.1	7.0 ± 0.1	1.00 × 10 <sup>−7</sup>	−6.3
4	( <i>p</i> -Cl)-Ph	0.23	16.1	7.3 ± 0.2	5.01 × 10 <sup>−8</sup>	−5.9
5	Ph	0.00	15.9	7.6 ± 0.1	2.51 × 10 <sup>−8</sup>	−5.5
6	( <i>p</i> -CH <sub>3</sub> )-Ph	−0.17	15.7	7.7 ± 0.1	2.00 × 10 <sup>−8</sup>	−5.3
7	( <i>p</i> -OH)-Ph	−0.37	15.3	8.0 ± 0.1	1.00 × 10 <sup>−8</sup>	−4.9
8	( <i>m</i> -NO <sub>2</sub> )-Ph	0.71	16.6	6.9 ± 0.1	1.25 × 10 <sup>−7</sup>	−6.4
9	( <i>m</i> -OH)-Ph	0.12	15.6	7.4 ± 0.2	5.01 × 10 <sup>−8</sup>	−5.9
10	( <i>o</i> -OH)-Ph	<i>na</i> <sup>b</sup>	15.1	6.9 ± 0.2	1.25 × 10 <sup>−7</sup>	−6.4
11	CH <sub>3</sub>	<i>na</i> <sup>b</sup>	14.5	8.2 ± 0.1	6.31 × 10 <sup>−9</sup>	−4.6
12	CF <sub>3</sub>	<i>na</i> <sup>b</sup>	18.4	6.1 ± 0.2	7.94 × 10 <sup>−7</sup>	−7.5

<sup>a</sup>Obtained from ref 27. <sup>b</sup>*na*: not applicable.

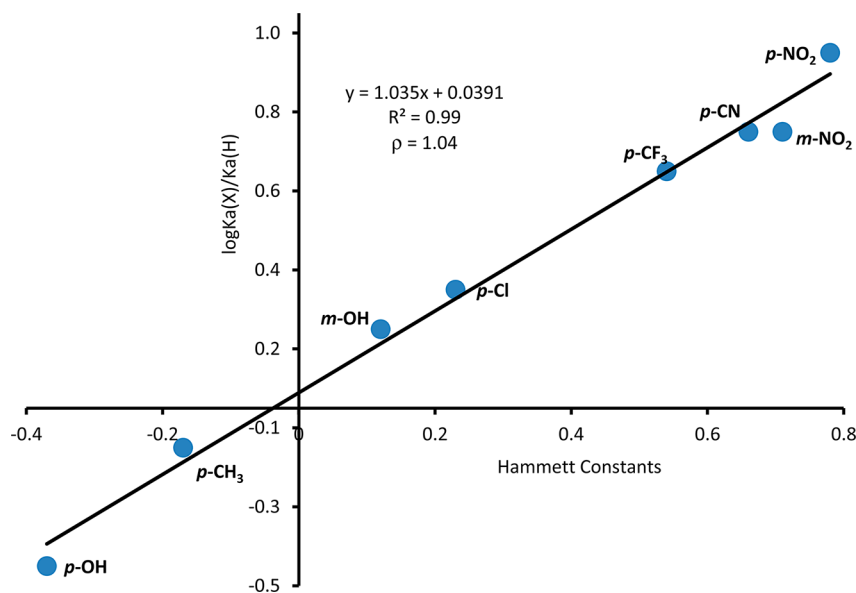


Figure 7. Hammett correlation of model system A.

that model system A might be a suitable system to investigate substituent effects. To determine the  $pK_a$  of the various acids prepared, we adopted the NMR method developed by Choi,<sup>24</sup> which is a modified version of similar procedure developed by Perrin et al.<sup>25</sup> The subsequently determined  $pK_a$  values for 1–12 in DMSO solutions are compiled in Table 1.

In DMSO, the stabilization of the conjugate monoanions by intramolecular hydrogen bonding acts to increase the acidity of the neutral acids in which the experimentally observed  $pK_a$  values ( $pK_{obs}$ ) are actually lower (i.e., more acidic) than their corresponding intrinsic values ( $pK_{int}$ ). The intrinsic  $pK_{int}$  refers to the  $pK_a$  of the carboxylic acids in the absence of the intramolecular hydrogen bonds.<sup>18</sup> The difference between  $pK_{obs}$  and  $pK_{int}$  provides a quantitative measure of intramolecular N–H $\cdots$ O hydrogen bond strength according to eq 1.

$$\Delta G = -RT \ln (K_{obs}/K_{int}) \quad (1)$$

The values for the  $pK_{int}$  were obtained by assuming that the measured  $pK_a$  of the control models (13–16) are equal to  $pK_{int}$ . This assumption has been validated.<sup>16,18,21,26</sup> An expected trend for the controls was that, in the absence of intramolecular hydrogen bonds, changes in the substituent groups had relatively little influence on their acidity because their  $pK_a$  values were observed to be within  $\pm 0.4$  unit. The average  $pK_a$  for 13–16 was 11.6; this value was used as an approximated  $pK_{int}$  value.

By comparing the experimental  $pK_a$  for 5 ( $7.6 \pm 0.1$ ) to the averaged values for the control model (11.6), it becomes apparent that a single amide (N–H $\cdots$ O) intramolecular hydrogen bond is capable of increasing the acidity of the benzoic acid by 5.5 kcal/mol ( $\Delta pK_a = \sim 4$  units). This energetic value is within the range of “moderate” hydrogen bonds.<sup>27</sup> However, the introduction of an electron-withdrawing group on the benzamide, such as the NO<sub>2</sub> (1), led to an increase in acidity relative to 5. By applying eq 1, the  $pK_a$  of  $6.7 \pm 0.2$  for 1 corresponds to a 6.7 kcal/mol hydrogen bond stabilization of the carboxylate. Thus, by implication, the NO<sub>2</sub> group has increased the strength of the single N–H $\cdots$ O intramolecular hydrogen bond by an additional 1.2 kcal/mol relative to 5. As expected, the electron-withdrawing groups can reduce the  $\pi$ -electron density of the aromatic ring, which in turn should polarize the N–H bond

toward a more positively charged proton. The polarization of the N–H bond might then lead to a stronger N–H $\cdots$ O hydrogen-bond interaction. Conversely, when the substituent was an electron-donating group (such as the OH group 7), a lowered acidity (i.e., higher  $pK_a$  of  $8.0 \pm 0.1$  relative to 5) was calculated, which indicates that the hydrogen bond strength in 5 is 0.6 kcal/mol stronger than in 7. On the other hand, compounds 11 and 12 are devoid of benzamide (aromatic) rings; the effects of the substituent groups in these examples are most likely transmitted by the inductive effect. Substituting the methyl group in 11 ( $pK_a = 8.2 \pm 0.1$ ) for a trifluoromethyl group as in 12 ( $pK_a = 7.0 \pm 0.2$ ) increased the acidity of 12 by 2.9 kcal/mol per hydrogen bond relative to 11. This represents the most significant increase in the hydrogen bond free energy in A series of compounds.

The energetic contributions of substituent groups might become significant in enzyme catalysis where the transition states can be stabilized by multiple hydrogen bonds to a single oxygen atom.<sup>28</sup> In this instance, if we assume that the contributions of the three N–H $\cdots$ O hydrogen bonds to the ester carbonyl are nearly additive, as previously proposed by Shan and Herschlag,<sup>16</sup> then it is possible to stabilize the transition state by an additional  $\sim 8.7$  kcal/mol (i.e.,  $3 \times 2.9$  kcal/mol) simply by tuning the individual hydrogen bonds with a strong electron-withdrawing group.

One way to trace the origin of substituent effects observed in model system A is to correlate the various hydrogen-bonding free energies with the respective Hammett constants.<sup>29,30</sup> The Hammett constant  $\sigma_p$  is generally recognized as describing the electron movement through the  $\sigma$ - and the  $\pi$ -frameworks caused by inductive and resonance effects, respectively.<sup>31</sup> In the original treatment of Hammett constants, ortho-substituted benzene derivatives were not included because of steric reasons. However, in model system A, one can assume that, because the carboxylates and the amide NH are hydrogen bonded, the two functional groups can be viewed as a composite unit in which the para substituents on the benzamide ring can electronically control the hydrogen-bond strength/acid ionization.

The values for the Hammett constants were obtained from ref 27, and the results are shown in Figure 7. A linear free-energy

relationship was obtained for the Hammett plot. The best-fit line originated from a near-zero intercept (0.04), which makes the Hammett plot consistent with eq 2. Consequently, the sensitivity of the substituent effect ( $\rho$ ) calculated as the slope gave a value of 1.04. By definition, such a  $\rho$  value suggests that substituent effects in the amide hydrogen bonds are comparable to the substituent effects observed for the ionization of benzoic acids derivatives in aqueous conditions. As a result, one can conclude that as the electron density of the phenyl ring decreases, both the energetics of N–H···O interaction and the ionizability of the carboxylic acid group increase.

$$\log[K_a(X)/K_a(H)] = \sigma\rho \quad (2)$$

As a result of the linear Hammett plot, it appears that, for model system **A**, the energetic contribution of any substituent to N–H···O hydrogen-bond interaction, and by extension to the acidity of the benzoic acid, can be predicted on the basis of their Hammett values. However, we caution that such an assumption might be an oversimplification and potentially misleading because the free energies of noncovalent interactions, especially those involving aromatic rings, tend to be sensitive to substituent positioning.<sup>32</sup> We note that, in addition to electronic contribution of substituent groups, these groups may also lead to significant secondary interactions through field effects,<sup>31,33</sup> or the so-called “local direct interactions”.<sup>34</sup> For instance, when we measured the acidity of **9** and **10** (which are isomers of **7**, shown in Figure 8),  $pK_a$  values of  $7.4 \pm 0.2$  and

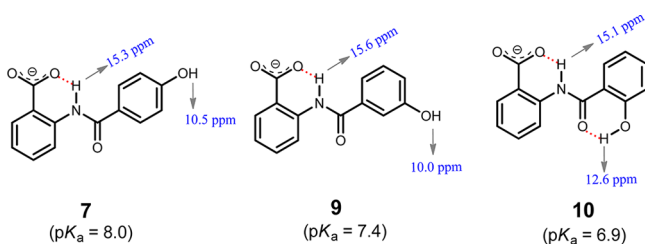


**Figure 8.** DFT-calculated structures at the B3LYP/6-31+G(d) levels. The selected chemical shifts were observed in  $^1\text{H}$  NMR. The H···O distance is 1.61 Å in **7**, 1.59 Å in **9**, and 1.58 Å in **10**.

$6.9 \pm 0.2$  were determined, respectively. This implies that **10** is about 1.5 kcal/mol more acidic than **7**. The higher acidity of **10** might result from the cumulative effect of the two conjugated hydrogen bonds. Positioning the hydroxyl group at the ortho carbon in **10** creates the possibility of forming a second “outer” hydrogen bond with the amide (as shown in Figure 8), which will compliment the “inner” N–H···O hydrogen bond in stabilizing the carboxylate. DFT calculations and proton NMR spectroscopy provided further support for this arrangement. In the DFT-optimized structures, the inner H···O distance in **10** was calculated to have the shortest distance, which suggests a stronger N–H···O hydrogen bond. Furthermore, as expected, the downfield chemical shifts of the bridging NH proton for **7**, **9**, and **10** were almost identical, (i.e., 15.3, 15.6, and 15.1 ppm, respectively). However, the corresponding OH chemical shift of **10** was 2.1 and 2.6 ppm more downfield than in **7** and **9**, respectively. With these results, it is therefore not completely unreasonable to infer that the higher acidity of **10** ( $\sim 1.5$  kcal/mol) relative to **7** is due to the additional ortho hydroxyl hydrogen bond. In fact, Kass et al. found similar effects in alcohols using a heptaol model compound.<sup>17</sup> However, to the best of our

knowledge, no quantitative measurements have been made for amide hydrogen bond.

Bearing in mind that **5** (with no substituents) has a  $pK_a$  of  $7.6 \pm 0.1$ , the observed  $pK_a$  value of  $7.4 \pm 0.2$  for **9** is consistent with the fact that meta-hydroxyl groups are actually electron-withdrawing; hence, the Hammett constant has a positive value ( $\sigma_m = +0.12$ ). On the other hand, hydroxyl groups at the para position (**7**) are strongly electron-donating ( $\sigma_p = -0.37$ ), indicating a resonance effect; therefore, the  $pK_a$  of  $8.0 \pm 0.1$  is in accord with the expected trend.

## CONCLUSION

The energy of hydrogen bonds in solution has been a central issue when discussing the roles of hydrogen bonding in assisting the known effects found in enzyme catalysis. In this study, we have demonstrated that substituent groups can bolster the strength of a single amide hydrogen bond up to 2.9 kcal/mol. This finding provides further support for the concept of the cumulative stabilization power of hydrogen bonds as proposed by Shan et al.<sup>18</sup> and Kass et al.<sup>17</sup> It could be possible that substituent groups might provide the missing link between moderately interacting hydrogen bonds and strong hydrogen bonds, where strong hydrogen bonds have been related to enzyme catalysis. Although the mechanism of enzyme catalysis has been previously linked to the elusive energetic attributes of the so-called LBHBs, the results of this study provided no support for “special” hydrogen bond free energy. In fact, in the monoanion of **12**, the appearance of a 18.4 ppm  $^1\text{H}$  chemical shift for the bridging NH proton clearly signals the occurrence of LBHB, however, the calculated hydrogen-bond free energy (7.5 kcal/mol) is less than the proposed 10–20 kcal/mol for LBHB.

Furthermore, because linear free energy relationships were observed for model system **A**, it appears that one can make a reasonable prediction of the substituent effect on amide hydrogen bonds based on the calculated sensitivity value ( $\rho = 1.04$ ) and Hammett  $\sigma$  constants. However, one should be mindful that the relative positions of the substituents are equally important. This point was demonstrated by comparing the observed  $pK_a$  values of **7**, **9**, and **10**, where the formation of an “outer” hydrogen bond in **10** seems to have strengthened the N–H···O interaction by an additional 1.5 kcal/mol. The findings in this work should be of particular importance to computational enzyme designers because it is crucial to retain the original geometry of an enzyme’s active site while trying to find ways of increasing its binding affinity through secondary substituent effects.

## EXPERIMENTAL SECTION

**General Procedure for the Preparation of Model Compounds.**<sup>35</sup> To a solution of anthranilic acid (1.1 mmol, 151 mg) in anhydrous THF (4 mL) was 1.0 mmol of the appropriate benzoyl chloride added at room temperature. After cooling the solution using ice–water bath, 1.5 mmol of triethylamine was added dropwise and reaction was stirred at room temperature for additional 4–12 h. The mixture was poured into a 20–30 mL cold solution of 1.0 M HCl, and precipitates were collected by filtration. Recrystallization from THF–hexane solution afforded the desired compound in quantitative yields.

**2-(4-Nitrobenzamido)benzoic acid<sup>36</sup> (1):**  $^1\text{H}$  NMR (600 MHz, dmsO)  $\delta$  13.67 (s, 1H), 12.20 (s, 1H), 8.58 (d,  $J = 8.3$  Hz, 1H), 8.39 (d,  $J = 8.0$  Hz, 2H), 8.14 (d,  $J = 8.5$  Hz, 2H), 8.02 (d,  $J = 7.9$  Hz, 1H), 7.65 (t,  $J = 7.8$  Hz, 1H), 7.22 (t,  $J = 7.6$  Hz, 1H).  $^{13}\text{C}$  NMR (151 MHz, dmsO)  $\delta$  170.3, 163.5, 149.9, 140.8, 140.5, 134.7, 131.7, 129.0, 124.6,

124.1, 120.8, 117.8. HRMS (EI-TOF)  $m/z$  calcd for  $C_{14}H_{10}O_5N_2$  [ $M^+$ ] 286.0590, found 286.0590

**2-(4-Cyanobenzamido)benzoic acid<sup>37</sup> (2):**  $^1H$  NMR (600 MHz, dmsO)  $\delta$  12.16 (s, 1H), 8.58 (d,  $J = 8.3$  Hz, 1H), 8.22–7.86 (m, 4H), 7.62 (t,  $J = 7.8$  Hz, 1H), 7.19 (t,  $J = 7.5$  Hz, 1H).  $^{13}C$  NMR (151 MHz, dmsO)  $\delta$  170.3, 163.7, 140.9, 138.9, 134.7, 133.4, 131.7, 128.3, 123.9, 120.7, 118.6, 117.6, 114.8. HRMS (EI-TOF)  $m/z$  calcd for  $C_{15}H_{11}N_2O_3$  [ $M + H$ ]<sup>+</sup> 267.0770, found 267.0777

**2-(4-(Trifluoromethyl)benzamido)benzoic acid<sup>38</sup> (3):**  $^1H$  NMR (500 MHz, dmsO)  $\delta$  12.24 (s, 1H), 8.66 (d,  $J = 7.7$  Hz, 1H), 8.15 (d,  $J = 7.8$  Hz, 2H), 8.07 (dd,  $J = 7.9$ , 1.5 Hz, 1H), 7.99 (d,  $J = 6.9$  Hz, 2H), 7.69 (t,  $J = 7.9$  Hz, 1H), 7.25 (t,  $J = 7.6$  Hz, 1H).  $^{13}C$  NMR (126 MHz, dmsO)  $\delta$  170.4, 164.0, 141.1, 138.8, 134.8, 132.4, 132.2, 131.7, 128.5, 126.5, 123.9, 120.7, 117.6. HRMS (EI-TOF)  $m/z$  calcd for  $C_{15}H_{10}F_3NO_3$  [ $M + H$ ]<sup>+</sup> 310.0691, found 310.0701

**2-(4-Chlorobenzamido)benzoic acid<sup>36</sup> (4):**  $^1H$  NMR (300 MHz, dmsO)  $\delta$  13.65 (s, 1H), 12.14 (s, 2H), 8.64 (dd,  $J = 8.4$ , 1.0 Hz, 2H), 8.03 (dd,  $J = 7.9$ , 1.6 Hz, 2H), 7.93 (d,  $J = 8.7$  Hz, 5H), 7.69–7.58 (m, 7H), 7.19 (td,  $J = 8.0$ , 1.2 Hz, 2H).  $^{13}C$  NMR (126 MHz, dmsO)  $\delta$  170.5, 164.1, 141.3, 137.5, 134.7, 133.7, 131.7, 129.5, 129.4, 123.6, 120.4, 117.2. HRMS (EI-TOF)  $m/z$  calcd for  $C_{14}H_{10}O_3NCl$  [ $M$ ]<sup>+</sup> 275.0349, found 275.0348.

**2-Benzamidobenzoic acid<sup>36</sup> (5):**  $^1H$  NMR (600 MHz, dmsO)  $\delta$  13.75 (s, 1H), 12.15 (s, 1H), 8.68 (dd,  $J = 8.4$ , 1.1 Hz, 1H), 8.03 (dd,  $J = 7.9$ , 1.6 Hz, 1H), 7.92 (dd,  $J = 7.0$ , 1.5 Hz, 2H), 7.67–7.59 (m, 2H), 7.56 (ddd,  $J = 6.7$ , 4.5, 1.3 Hz, 2H), 7.22–7.14 (m, 1H).  $^{13}C$  NMR (151 MHz, dmsO)  $\delta$  170.4, 165.1, 141.6, 135.0, 134.8, 132.6, 131.7, 129.7, 129.4, 129.0, 127.4, 123.4, 120.3, 116.9.

**2-(4-Methylbenzamido)benzoic acid<sup>39</sup> (6):**  $^1H$  NMR (500 MHz, dmsO)  $\delta$  12.15 (s, 1H), 8.73 (d,  $J = 8.1$  Hz, 1H), 8.06 (d,  $J = 7.9$  Hz, 1H), 7.85 (d,  $J = 8.1$  Hz, 2H), 7.65 (t,  $J = 7.9$  Hz, 1H), 7.38 (d,  $J = 7.9$  Hz, 2H), 7.19 (t,  $J = 7.6$  Hz, 1H), 2.39 (s, 4H).  $^{13}C$  NMR (126 MHz, dmsO)  $\delta$  170.5, 165.0, 142.7, 141.8, 134.8, 132.2, 131.7, 129.9, 127.5, 123.2, 120.2, 116.7, 21.5.

**2-(4-Hydroxybenzamido)benzoic acid<sup>36</sup> (7):**  $^1H$  NMR (500 MHz, dmsO)  $\delta$  13.67 (s, 1H), 12.06 (s, 2H), 10.25 (s, 2H), 8.72 (d,  $J = 8.4$  Hz, 2H), 8.05 (dd,  $J = 7.9$ , 1.5 Hz, 1H), 7.82 (d,  $J = 8.7$  Hz, 2H), 7.72–7.61 (m, 1H), 7.23–7.10 (m, 1H), 6.92 (d,  $J = 8.7$  Hz, 2H).  $^{13}C$  NMR (126 MHz, dmsO)  $\delta$  170.6, 164.9, 161.5, 142.0, 134.7, 131.7, 129.6, 125.5, 122.9, 120.1, 116.6, 116.0. HRMS (EI-TOF)  $m/z$  calcd for  $C_{14}H_{12}NO_4$  [ $M + H$ ]<sup>+</sup> 258.0766, found 258.0761

**2-(3-Nitrobenzamido)benzoic acid<sup>40</sup> (8):**  $^1H$  NMR (500 MHz, dmsO)  $\delta$  12.33 (s, 9H), 8.84–8.81 (m, 1H), 8.72 (t,  $J = 1.9$  Hz, 5H), 8.61 (dd,  $J = 8.4$ , 1.0 Hz, 6H), 8.54 (ddd,  $J = 7.8$ , 1.6, 1.0 Hz, 1H), 8.49–8.45 (m, 7H), 8.35 (ddd,  $J = 7.8$ , 1.7, 1.0 Hz, 6H), 8.17–8.14 (m, 1H), 8.04 (dd,  $J = 8.0$ , 1.5 Hz, 6H), 7.96 (ddd,  $J = 8.1$ , 7.3, 1.5 Hz, 1H), 7.91–7.85 (m, 7H), 7.67 (ddd,  $J = 8.5$ , 7.4, 1.7 Hz, 7H), 7.24 (ddd,  $J = 7.9$ , 7.4, 1.2 Hz, 6H).  $^{13}C$  NMR (126 MHz, dmsO)  $\delta$  170.5, 162.9, 158.9, 154.9, 148.5 (d,  $J = 10.3$  Hz), 146.2, 140.9, 136.3, 133.8, 131.7, 131.2, 127.1, 124.0, 122.7–122.2 (m), 120.7, 117.7. HRMS (EI-TOF)  $m/z$  calcd for  $C_{14}H_{10}O_5N_2$  [ $M + H$ ]<sup>+</sup> 286.06680, found 286.0671.

**2-(3-Hydroxybenzamido)benzoic acid<sup>41</sup> (9):**  $^1H$  NMR (500 MHz, dmsO)  $\delta$  12.15 (s, 1H), 9.98 (s, 1H), 8.71 (dd,  $J = 8.4$ , 0.9 Hz, 1H), 8.05 (dd,  $J = 7.9$ , 1.6 Hz, 1H), 7.65 (ddd,  $J = 8.6$ , 7.4, 1.6 Hz, 1H), 7.43–7.34 (m, 3H), 7.24–7.15 (m, 1H), 7.08–6.99 (m, 1H).  $^{13}C$  NMR (126 MHz, dmsO)  $\delta$  170.4, 165.2, 158.3, 141.6, 136.4, 134.7, 131.7, 130.5, 123.3, 120.2, 119.7, 117.7, 117.0–116.4 (m), 114.5. HRMS (EI-TOF)  $m/z$  calcd for  $C_{14}H_{12}NO_4$  [ $M + H$ ]<sup>+</sup> 258.0766, found 258.0764.

**2-(2-Hydroxybenzamido)benzoic acid<sup>42</sup> (10):**  $^1H$  NMR (500 MHz,  $cd_3od$ )  $\delta$  8.75 (dd,  $J = 8.5$ , 1.0 Hz, 1H), 8.14 (dd,  $J = 8.0$ , 1.6 Hz, 1H), 7.84 (dd,  $J = 8.4$ , 1.6 Hz, 1H), 7.61 (ddd,  $J = 8.6$ , 7.4, 1.7 Hz, 1H), 7.45 (ddd,  $J = 8.3$ , 7.4, 1.6 Hz, 1H), 7.19 (ddd,  $J = 8.1$ , 7.3, 1.2 Hz, 1H), 6.99–6.92 (m, 2H).  $^{13}C$  NMR (126 MHz,  $cd_3od$ )  $\delta$  170.3, 168.5, 161.1, 140.7, 134.1, 133.9, 131.3, 126.8, 122.9, 120.4, 118.9, 117.7, 116.5, 115.6. HRMS (EI-TOF)  $m/z$  calcd for  $C_{14}H_{12}NO_4$  [ $M + H$ ]<sup>+</sup> 258.0766, found 258.0765.

**2-Acetamidobenzoic acid<sup>40</sup> (11):**  $^1H$  NMR (500 MHz, dmsO)  $\delta$  11.05 (s, 1H), 8.55–8.38 (m, 1H), 7.96 (dd,  $J = 7.9$ , 1.6 Hz, 1H), 7.56

(d,  $J = 1.3$  Hz, 1H), 7.26–6.99 (m, 1H), 2.12 (s, 3H).  $^{13}C$  NMR (126 MHz, dmsO)  $\delta$  169.9, 168.9, 141.3, 134.4, 131.5, 123.0, 120.4, 116.9, 25.4.

**2-(Trifluoroacetamido)benzoic acid<sup>40</sup> (12):**  $^1H$  NMR (600 MHz, dmsO)  $\delta$  13.67 (s, 1H), 12.43 (s, 1H), 8.24 (d,  $J = 8.1$  Hz, 2H), 8.01 (d,  $J = 7.6$  Hz, 2H), 7.66 (t,  $J = 7.5$  Hz, 2H), 7.31 (t,  $J = 7.4$  Hz, 2H).  $^{13}C$  NMR (126 MHz, dmsO)  $\delta$  169.8, 154.7 (m,  $J = 36.6$  Hz), 138.0, 134.7, 131.7, 125.8, 121.6, 119.5, 116.0 (m,  $J = 288.9$  Hz).

**4-(4-Nitrobenzamido)benzoic acid<sup>43</sup> (13):**  $^1H$  NMR (500 MHz, dmsO)  $\delta$  12.79 (s, 1H), 10.83 (s, 1H), 8.38 (d,  $J = 8.9$  Hz, 1H), 8.20 (d,  $J = 8.9$  Hz, 1H), 7.94 (dd,  $J = 23.7$ , 8.9 Hz, 2H).  $^{13}C$  NMR (126 MHz, dmsO)  $\delta$  167.3, 164.8, 151.0–149.8, 143.2, 140.7, 130.8, 129.8, 126.5, 124.0, 120.1.

**4-Benzamidobenzoic acid<sup>44</sup> (14):**  $^1H$  NMR (500 MHz, dmsO)  $\delta$  10.53 (s, 1H), 7.99–7.95 (m, 1H), 7.93 (d,  $J = 2.9$  Hz, 1H), 7.64–7.60 (m, 1H), 7.57–7.52 (m, 1H).  $^{13}C$  NMR (126 MHz, dmsO)  $\delta$  167.4, 166.4, 143.8, 135.8–135.2 (m), 132.3, 130.7, 128.9, 128.2, 125.9, 119.9.

**4-Acetamidobenzoic acid<sup>39</sup> (15):**  $^1H$  NMR (500 MHz, dmsO)  $\delta$  10.23 (s, 1H), 7.88 (d,  $J = 8.8$  Hz, 2H), 7.69 (d,  $J = 8.8$  Hz, 2H), 2.08 (s, 3H).  $^{13}C$  NMR (126 MHz, dmsO)  $\delta$  169.3, 167.4, 143.8, 130.8, 125.3, 118.6, 24.6.

**4-(2,2,2-Trifluoroacetamido)benzoic acid<sup>45</sup> (16):**  $^1H$  NMR (300 MHz, dmsO)  $\delta$  13.20–12.80 (br s, 1H), 11.51 (s, 1H), 7.88 (dd,  $J = 50.8$ , 8.2 Hz, 6H).  $^{13}C$  NMR (126 MHz, dmsO)  $\delta$  167.1, 155.2 (m), 140.8, 130.8, 128.02, 121.4–121.0 (m), 116.1 (m).

**Measurement of Ionization Constants in DMSO.** In a typical running, equimolar amounts of a test acid AH (in this case 1–11 with unknown  $pK_a$ ) and a conjugate acid B (a standard acid BH with known  $pK_a$ ) are combined in solution in an NMR tube. The resulting changes in the chemical shifts of the reporter nucleus ( $^1H$  or  $^{13}C$ ) were used to judge the position of equilibrium between the two acids. Because this method is a relative measure of the acids' strengths between AH and BH, the chemical shifts of the two acids ( $\delta_{AH}$  and  $\delta_{BH}$ ) and their corresponding monoanions ( $\delta_A$  and  $\delta_B$ ) must be known. Equation 3 describes the relationship between the chemical shifts and the ionization constants of the two acids used. The unknowns in eq 3 are the equilibrium chemical shifts for when AH and B<sup>−</sup> or A<sup>−</sup> and BH are mixed together, i.e.,  $\delta_a$  and  $\delta_b$ , respectively. The advantage of this technique over others are that (1) only a single measurement, which can be repeated many times if desired, is required in order to determine the acidity ( $K_a$ ) of the unknown compound, and (2) the standard measurement approach ensures that the ionization equilibrium is restricted only to the first deprotonation step because the model systems used in this study have more than one readily ionizable proton. The best results for using eq 3 are obtained when AH and BH are separated by  $\sim 2$   $pK_a$  units. *p*-Bromobenzoic acid ( $pK_a = 10.5$ ), *p*-nitrobenzoic acid ( $pK_a = 9.1$ ), and salicylic acid ( $pK_a = 6.6$ ) were used as the standard BH acids in DMSO solution.

$$K_a(\delta_a - \delta_A)(\delta_{BH} - \delta_b) = K_b(\delta_b - \delta_B)(\delta_{AH} - \delta_a) \quad (3)$$

**Preparation of Samples in DMSO.** The monoanion salts were prepared by mixing a  $CH_3OH$  solution of the appropriate acid with 1 equiv of tetrabutylammonium hydroxide solution (1.0 M in  $CH_3OH$ ) respectively. Both  $H_2O$  and  $CH_3OH$  were subsequently removed by evaporation under reduced pressure, followed by heating the sample ( $\sim 70$  °C) for 1–2 h under high vacuum to yield solids. In cases where an oily product persists after heated drying, the product is dissolved in minimum THF, and the solid product is precipitated with hexanes. Dried samples were then stored in a positive pressure glovebox for subsequent use. The solute concentration used for NMR analysis in 99.9% DMSO- $d_6$  was about 0.01 M or less for all samples.

**Spectra Measurements.** NMR spectra were recorded with a 300 MHz NMR spectrometer using the default pulse sequence in the software. Typical spectra parameters for  $^1H$  spectra: 16 scans, spectral width 9600 Hz, relaxation delay of 1 s, and acquisition time of 4 s. Unless otherwise stated, all measurements were at a regulated temperature of 25 °C.

**Theoretical Calculations.** Conformational distributions were performed using the SPARTAN '08 program. The selected pre-optimized conformers were then fully optimized by DFT methods

using the Gaussian09 package.<sup>46</sup> All energy minima were verified to have 0 imaginary frequencies by vibrational frequency analysis.

## ■ ASSOCIATED CONTENT

### ● Supporting Information

Cartesian coordinates of the optimized structures used in the theoretical conformational analysis and the crystallographic data (cif) for compound 1. This material is available free of charge via the Internet at <http://pubs.acs.org>.

## ■ AUTHOR INFORMATION

### Corresponding Author

\*robertsj@caltech.edu

### Notes

The authors declare no competing financial interest.

## ■ ACKNOWLEDGMENTS

Acknowledgement is made to the National Science Foundation under Grants CHE-0841550, TG-CHE1000106, and to the donors of the Petroleum Research Fund administered by the American Chemical Society for support for this research. Other important support came from the Summer Undergraduate Research Fellowship Program (SURF) at the California Institute of Technology, the Senior Scientist Mentor Program of the Camille and Henry Dreyfus Foundation, and the NORAC Grant to Caltech by Dr. and Mrs. Chester M. McCloskey. We are indebted to Merck and Company, Dr. David J. Mathre, and Edith M. Roberts for their helpful financial assistance. The facilities of the MCS used in these studies were established with grants from DURIP-ONR and DURIP-ARO, with additional support from ONR, ARO, NSF, NIH, DOE, Chevron, Nissan, Dow Corning, Intel, Pfizer, Boehringer-Ingelheim, and Sanofi-Aventis.

## ■ REFERENCES

- (1) Jencks, W. P. *Adv. Enzymol. Relat. Areas Mol. Biol.* **1975**, *43*, 219.
- (2) Jencks, W. P. *Acc. Chem. Res.* **1976**, *9*, 425.
- (3) Reed, G. H.; Poyner, R. R.; Larsen, T. M.; Wedekind, J. E.; Rayment, I. *Curr. Opin. Struct. Biol.* **1996**, *6*, 736.
- (4) Richard, J. P. *Biochemistry* **2012**, *51*, 2652.
- (5) Gerlt, J. A.; Kreevoy, M. M.; Cleland, W. W.; Frey, P. A. *Chem. Biol.* **1997**, *4*, 259.
- (6) Usher, K. C.; Remington, S. J.; Martin, D. P.; Drueckhammer, D. G. *Biochemistry* **1994**, *33*, 7753.
- (7) Gu, Z. T.; Drueckhammer, D. G.; Kurz, L.; Liu, K.; Martin, D. P.; McDermott, A. *Biochemistry* **1999**, *38*, 8022.
- (8) Cassidy, C. S.; Lin, J.; Frey, P. A. *Biochemistry* **1997**, *36*, 4576.
- (9) Perrin, C. L. *Acc. Chem. Res.* **2010**, *43*, 1550.
- (10) Guthrie, J. P. *Chem. Biol.* **1996**, *3*, 163.
- (11) Warshel, A.; Sharma, P. K.; Kato, M.; Xiang, Y.; Liu, H. B.; Olsson, M. H. M. *Chem. Rev.* **2006**, *106*, 3210.
- (12) Schutz, C. N.; Warshel, A. *Proteins: Struct., Funct., Bioinf.* **2004**, *55*, 711.
- (13) Chen, J. G.; McAllister, M. A.; Lee, J. K.; Houk, K. N. *J. Org. Chem.* **1998**, *63*, 4611.
- (14) Kolonko, K. J.; Reich, H. J. *J. Am. Chem. Soc.* **2008**, *130*, 9668.
- (15) Kato, Y.; Toledo, L. M.; Rebek, J. *J. Am. Chem. Soc.* **1996**, *118*, 8575.
- (16) Shan, S. O.; Herschlag, D. *J. Am. Chem. Soc.* **1996**, *118*, 5515.
- (17) Shokri, A.; Abedin, A.; Fattahi, A.; Kass, S. R. *J. Am. Chem. Soc.* **2012**, *134*, 10646.
- (18) Shan, S. O.; Loh, S.; Herschlag, D. *Science* **1996**, *272*, 97.
- (19) Mori, N.; Asano, Y.; Irie, T.; Tsuzuki, Y. *Bull. Chem. Soc. Jpn.* **1969**, *42*, 482.

- (20) Nagy, P. I.; Dunn, W. J.; Alagona, G.; Ghio, C. *J. Phys. Chem.* **1993**, *97*, 4628.
- (21) Shi, Z. S.; Krantz, B. A.; Kallenbach, N.; Sosnick, T. R. *Biochemistry* **2002**, *41*, 2120.
- (22) Rudner, M. S.; Jeremic, S.; Petterson, K. A.; Kent, D. R.; Brown, K. A.; Drake, M. D.; Goddard, W. A.; Roberts, J. D. *J. Phys. Chem. A* **2005**, *109*, 9076.
- (23) Markley, J. L. *Biochemistry* **1978**, *17*, 4648.
- (24) Choi, P. J.; Petterson, K. A.; Roberts, J. D. *J. Phys. Org. Chem.* **2002**, *15*, 278.
- (25) Perrin, C. L.; Fabian, M. A. *Anal. Chem.* **1997**, *69*, 108.
- (26) Pinto, S. S.; Diogo, H. P.; Guedes, R. C.; Cabral, B. J. C.; da Piedade, M. E. M.; Simoes, J. A. M. *J. Phys. Chem. A* **2005**, *109*, 9700.
- (27) Mariam, Y. H.; Musin, R. N. *J. Phys. Chem. A* **2008**, *112*, 134.
- (28) Zhang, Y. K.; Kua, J.; McCammon, J. A. *J. Am. Chem. Soc.* **2002**, *124*, 10572.
- (29) Hammett, L. P. *J. Am. Chem. Soc.* **1937**, *59*, 96.
- (30) Hansch, C.; Leo, A.; Taft, R. W. *Chem. Rev.* **1991**, *91*, 165.
- (31) Roberts, J. D.; Moreland, W. T. *J. Am. Chem. Soc.* **1953**, *75*, 2167.
- (32) Gung, B. W.; Emenike, B. U.; Alvarez, C. N.; Rakovan, J.; Kirschbaum, K.; Jain, N. *Tetrahedron Lett.* **2010**, *51*, 1648.
- (33) Roberts, J. D.; Carboni, R. A. *J. Am. Chem. Soc.* **1955**, *77*, 5554.
- (34) Wheeler, S. E.; Houk, K. N. *J. Am. Chem. Soc.* **2008**, *130*, 10854.
- (35) Wiklund, P.; Bergman, J. *Tetrahedron Lett.* **2004**, *45*, 969.
- (36) Prashanth, M. K.; Revanasiddappa, H. D. *Med. Chem. Res.* **2013**, *22*, 2665.
- (37) Shultz, P.; Bouchez, L. PCT Int. Appl. WO/2012/129562 A2 20120927, 2012.
- (38) Hamprecht, G.; Rohr, W.; Varwig, J.; Wuerzer, B. Ger. Offen DE 3308239 A1 19840913, 1984.
- (39) Zentmyer, D. T.; Wagner, E. C. *J. Org. Chem.* **1949**, *14*, 967.
- (40) Errede, L. A.; Oien, H. T.; Yarian, D. R. *J. Org. Chem.* **1977**, *42*, 12.
- (41) Sinreih, M.; Sosic, I.; Beranic, N.; Turk, S.; Adeniji, A. O.; Penning, T. M.; Rizner, T. L.; Gobec, S. *Bioorg. Med. Chem. Lett.* **2012**, *22*, 5948.
- (42) Hauteville, M.; Ponchet, M.; Ricci, P.; Favrebonvin, J. *J. Heterocycl. Chem.* **1988**, *25*, 715.
- (43) Abbel, R.; Frey, H.; Schollmeyer, D.; Kilbinger, A. F. M. *Chem.—Eur. J.* **2005**, *11*, 2170.
- (44) Zheng, C. H.; Yang, H.; Zhang, M.; Lu, S. H.; Shi, D.; Wang, J.; Chen, X. H.; Ren, X. H.; Liu, J.; Lv, J. G.; Zhu, J.; Zhou, Y. *J. Bioorg. Med. Chem. Lett.* **2012**, *22*, 39.
- (45) Ban, H.; Gavriluk, J.; Barbas, C. F. *J. Am. Chem. Soc.* **2010**, *132*, 1523.
- (46) Frisch, M. J.; et al. *Gaussian09*; Gaussian, Inc.: Wallingford CT, 2009.